DOI 10.5162/EUROSENSORSXXXVI/OT5.232

Raman Spectroscopy-based Detection of Suspended Carbon Nanotubes for Integration into Sensors

N. Monnerat[1], I. Kraiem[1], C. Roman [1], C. Hierold[1], M. Haluska[1]
[1] *Micro- and Nanosystems D-MAVT ETH Zürich, Tannenstrasse 3,8092 Zürich, Switzerland*

Haluskam@ethz.ch

In this study, the visualization of CVD grown suspended CNTs intended for individual carbon nanotube field effect transistor gas sensors was investigated. Two visualization techniques were compared: SEM and Raman spectroscopy. By comparing the CNT visibility by the 514 nm laser wavelength of Raman spectroscopy to the CNT visibility in SEM, a detection yield of 90.3% by Raman was determined. For the CNT detectability by Raman, both G and D* Raman bands were considered.

SWCNT for sensors, CNFET gas sensors, Raman spectroscopy, SEM, Detection yield

Visualizing Carbon Nanotubes

Carbon Nanotubes (CNTs) offer a vast array of potential applications due to their exceptional electronic, mechanical, and thermal properties [1]. Single-walled CNTs (SWCNTs) for example are particularly promising because of their low detection limit of different gases including NO_2 [2].

Different approaches address the challenge of integrating individual CNTs into device structures, including dielectrophoresis (wet transfer) [3], and dry mechanical transfer techniques [4]. Wet transfer techniques come with a high risk of contamination. Dry transfer requires prelocalization of CNTs before their integration into sensors.

Several techniques can visualize as-grown individual CNTs. SEM can, in principle, detect all CNTs. However, M. Muoth et al [4] reported electrical degradation of CNTs post-SEM.

On the other hand, Raman spectroscopy allows for non-destructive detection of individual suspended CNTs [5]. In addition, it can provide information on the structural and electrical properties of CNTs. The downside of Raman imaging is an expected lower CNT detection yield compared to SEM.

This study was motivated by the scarcity of research on the suspended CNT detection yield by Raman spectroscopy.

Samples and Measurement Methods

CNTs used in this work have expected diameters ranging from 1.5 to 2.5 nm and were synthesized by chemical vapor deposition in CH_4/H_2 atmosphere using an iron-based catalyst precursor [6].

All Raman measurements were conducted by the Renishaw InVia Qontor System using the StreamLine™ scanning method with an elliptical laser beam and a wavelength of 514 nm. The microscope objective had an NA of 0.75 and a magnification of 50x. The optical depth of focus allowed to detect tubes at full sample-depth (5 µm).

The CNTs were manually counted in spectral maps filtered by the G (around 1585 cm^{-1}) and D* (around 2665 cm^{-1}) bands. These bands, seen in Fig. 1., only materialize when the so-called resonance condition for incoming or outgoing (scattered) light is fulfilled [5]. Otherwise, the bands do not appear in Raman spectra and the CNT can't be detected, as seen in Fig. 2.

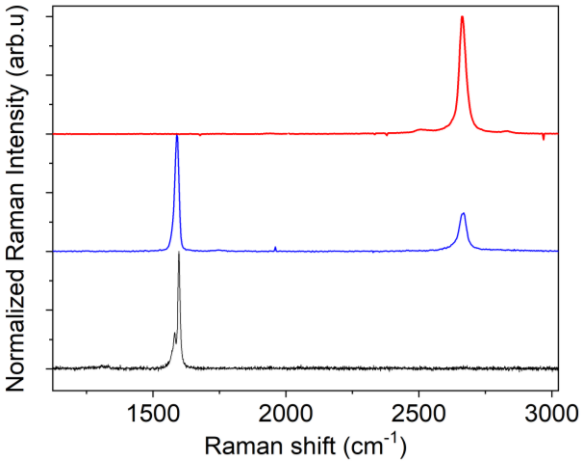

Fig. 1. Vertically shifted Raman spectra of three CNTs with differently visible G (left) and D (right) bands. The spectra are normalized at the dominant peak.*

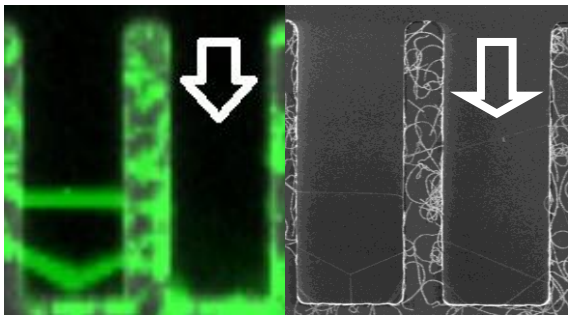

Fig. 2. The same two trenches in a Raman measurement map (left) and in a SEM image (right). The green color shows the CNTs visible by Raman. The white arrows point to a SEM-visible CNT that is invisible in 514nm-Raman spectroscopy.

Results

1676 SEM-visible CNTs were investigated by Raman and the detection yields with a Raman laser wavelength of 514nm were determined and summarized in Table 1. In maps filtered by the G band, 85.3% (1429) of CNTs were visible. An additional 5% (84) of CNTs were only visible in D* band filtered maps, raising the CNT detection yield to 90.3%.

Tab. 1: Yield values of visible CNTs

	Amount of visible CNTs	CNT detection yield
SEM	1676	100%
G band	1429	85.3%
only D* band	84	5%

Discussion

The experimental results can be compared to theoretical expectations based on the Kataura plot [7], which are summarized in Table 2 for three different CNT diameter distributions and distribution types.

Tab. 2: Theoretical CNT visibility in Raman spectroscopy based on the Kataura Plot [7].

	Ø 1.9 ± 0.27 nm Gaussian	Ø 0.7-3.5 nm Uniform	Ø 3.2 ± 0.45 nm Gaussian
G band	54.4%	61.9%	77.9%
only D* band	15%	13.9%	13.3%

The experimental detection yield obtained by the 514 nm Raman spectroscopy is higher than the theoretical values. Several reasons might contribute to this difference: one is the counting practice. Possible CNT bundles were counted as one CNT in SEM and as one CNT in Raman maps if two or more Radial Breathing Modes (RBM) were not simultaneously detected. The occurrence of more CNTs in a bundle increases the probability of detecting minimally one of them in a Raman map, thus increasing the Raman yield in respect to SEM count. The same issue arises with multi-walled CNTs. Another reason may be that investigated CNTs possess other diameter distributions than expected. For example, the fourth column of Tab. 2. shows a significant increase in the Raman detection yield if the diameter distribution is shifted to larger values and is broader at the same time.

In conclusion, this study shows that Raman spectroscopy is a good alternative for visualizing/detecting CNTs before their integration into sensor devices. The CNT detection yield by Raman spectroscopy is slightly lower than that of SEM. Nonetheless, Raman spectroscopy is much gentler to the CNTs than SEM, that was shown to significantly affect the properties of exposed CNTs. Raman also gives additional information about the CNTs, such as their electrical conductivity type, thus enabling selection of CNTs with the right properties for functional CNFET sensors.

We would like to thank R. Stirnimann for his help with Raman spectroscopy, and L. Schürz for sample preparation, as well as the MNS & BRNC teams for making this research possible.

References

[1] N. Popov, Carbon nanotubes: properties and application, Materials Science and Engineering: R: Reports 43.3, 61-102 (2004); doi: 1016/j.mser.2003.10.001

[2] K. Chikkadi et al, Beilstein J. Nanotech., 5, 2179–2191 (2014);doi :0.3762/bjnano.5.227

[3] W. Li et al, “Principles of carbon nanotube dielectrophoresis,” Nano Research, vol. 14, pp. 2188–2206, 2021. Publisher: Springer; doi : 10.1007/s12274-020-3183-0

[4] M. Muoth et al, Transfer of carbon nanotubes onto microactuators for hysteresis-free transistors at low thermal budget, 2012 IEEE 25th International Conference on Micro Electro mechanical Systems (MEMS), pp. 1352-1355 (2012); doi: 10.1109/MEMSYS.2012.6170417.

[5] M.S. Dresselhaus et al, Raman spectroscopy of carbon nanotubes. Physics Reports, 409(2):47–99 (2005); doi: 10.1016/j.physrep.2004.10.00

[6] L. Durrer et al, Nanotech., 20 35560 (2009); doi: 10.1088/0957-4484/20/35/355601

[7] K. Liu et al, An atlas of carbon nanotube optical transitions. Nature Nanotech 7, 325–329 (2012); doi: 10.1038/nnano.2012.52